GEOPHYSICAL RESEARCH LETTERS, VOL. 22, NO. 6, PAGES 675-678, MARCH 15, 1995

# Comparison of empirical magnetic field models and global MHD simulations: The near-tail currents

T. I. Pulkkinen
Finnish Meteorological Institute, Helsinki, Finland

D. N. Baker[1]
NASA Goddard Space Flight Center, Greenbelt, MD

R. J. Walker, J. Raeder, and M. Ashour-Abdalla
Institute of Geophysics and Planetary Physics, University of California, Los Angeles, CA

**Abstract.** The tail currents predicted by empirical magnetic field models and global MHD simulations are compared. It is shown that the near-Earth currents obtained from the MHD simulations are much weaker than the currents predicted by the Tsyganenko models, primarily because the ring current is not properly represented in the simulations. On the other hand, in the mid-tail and distant tail the lobe field strength predicted by the simulations is comparable to what is observed at about $50R_E$ distance, significantly larger than the very low lobe field values predicted by the Tsyganenko models at that distance. Ways to improve these complementary approaches to model the actual magnetospheric configuration are discussed.

## Introduction

The inner magnetotail is an interesting transition region where the tail-like magnetic field and thin plasma sheet change to a quasi-dipolar field configuration. Recent observations have shown that the inner edge of the plasma sheet is very active at, and immediately after, the substorm onset (thinning of the plasma sheet prior to onset, current sheet disruption, and magnetic field dipolarization simultaneously with ground onset signatures). Several authors have thus proposed that processes in this region initiate the substorm onset [see, e.g., Baker and Pulkkinen, 1991].

The field line configuration changes in the global MHD simulations after the southward turning of the IMF (including formation and tailward ejection of plasmoids) have supported the near-Earth neutral line model (NENL) for substorms. The formation of the neutral line and its location in the tail have recently been key questions in substorm research [e.g., Baker and Pulkkinen, 1991]. Furthermore, the relation of the neutral line formation to the near-Earth current sheet disruption observations is still under debate.

The current and field configurations, especially the distribution of $B_Z$ along the tail, determine through which instability the energy stored in the magnetotail is released during the substorm expansion phase. Thus, the key problems in substorm studies are (1) to determine the location of the instability in the tail, and (2) to determine the field and current distributions at that location. This effort requires comparison of data analyses and complementary modeling approaches in various parts of the tail.

In this paper we compare empirical magnetic field models developed based on the Tsyganenko [1989] models (T89) [Pulkkinen et al., 1992] with the magnetic field configuration and currents obtained from global MHD simulations [Raeder et al., 1994; Raeder, 1994; Walker et al., 1993]. Especially, we examine the behavior of the near-tail currents both during magnetically quiet times and during the substorm evolution.

## Quiet time configuration

The T89 models describe the inner magnetotail currents with two near-equatorial current systems: The "ring current" encircling the Earth (current maximum inside $10R_E$) and the "tail current" mainly in the cross-tail direction (current maximum outside $10R_E$). Figure 1a shows the $Z$-integrated current (in mA/m) from the T89 model for different levels of magnetic activity. Note that mainly the near-Earth ring current increases as a function of magnetic activity; changes in the tail current are much smaller (Figure 1b). Figure 1c shows the $Z$-integrated current from two MHD simulations: The solid curve shows the current from a simulation run after 90 min of pure southward IMF ($B_Z = -5$ nT, $V_X = 500$ km/s, $n = 13$ cm$^{-3}$, $T = 3 \cdot 10^5$ K) followed by 73 min of IMF data from IMP 8 from a period with mostly northward $B_Z$ [Raeder, 1994]. The dashed curve shows the current after 4 hours of pure northward IMF ($B_Z = 5$ nT, $V_X = 400$ km/s, $n = 6.75$ cm$^{-3}$, $T = 0.5 \cdot 10^5$ K) [Raeder et al., 1994]. The currents have been calculated numerically from the mag-

[1]Now at Laboratory for Atmospheric and Space Physics, University of Colorado, Boulder, CO



**Paper number 95GL00540**
**0094-8534/95/95GL-00540$03.00**

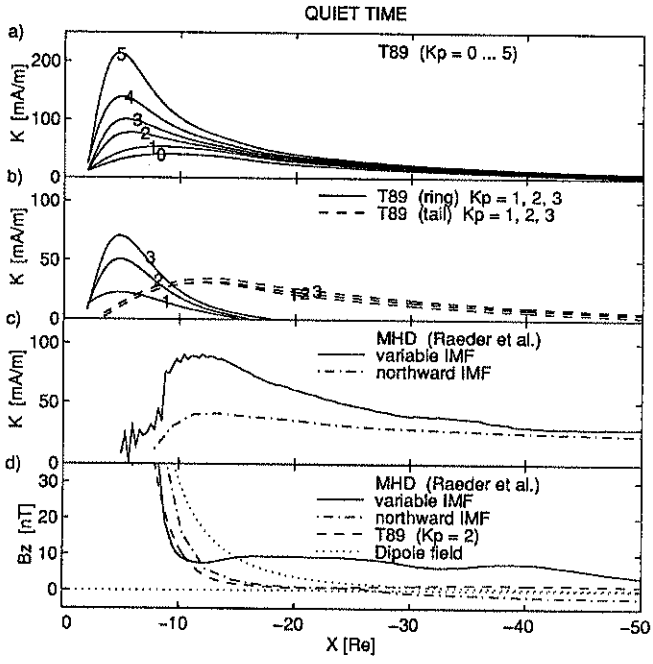


**Figure 1** a) Integrated currents from the T89 model at $Y = 0$ for different levels of magnetic activity (dipole tilt angle zero). b) Same as in (a), but the ring current and tail current terms are shown separately. c) Integrated currents from the simulations during variable IMF (solid line) and during northward IMF (dashed line) [Raeder et al., 1994; Raeder, 1994]. d) $B_Z$ along tail axis from pure dipole (dotted line), from the simulations during variable IMF (solid line) and during northward IMF (dash-dotted line), and from the T89 $Kp = 2$ model for (dashed line).

netic field values using $K = \int dz\ \nabla \cdot \mathbf{B}/\mu_0$, where the integration extends over the plasma sheet thickness.

Both the T89 and MHD models show clear dependence on previous magnetic activity in the near-Earth region. The current maximum in the MHD model under northward IMF is comparable to the quietest versions of the T89 models, whereas the current maximum after southward IMF in the simulation is close to the T89 ($Kp = 3$) model. In both simulation runs, the current maximum is located further from the Earth than in the T89 models.

The most significant difference between the empirical and MHD current profiles is the lack of a strong near-Earth current maximum in the MHD model. Division of the T89 model currents into ring and tail current components (Figure 1b) clearly shows that the ring current is not properly represented in the MHD simulations. This may be due to the fact that the ring current formation involves non-MHD processes. Also, the large size of the ionosphere ($\sim 3.5 R_E$) in the simulation may limit the validity of the near-Earth description.

The current intensity in the simulations assumes an almost constant value ($\sim$25 mA/m) tailward of about $30 R_E$. The T89 models suggest a much more rapid decay of the current intensity as the radial distance from the Earth increases, giving only 9 mA/m at $40 R_E$ and 5 mA/m at $50 R_E$. The observations give about 33 mA/m at $30 R_E$, 25 mA/m at $50 R_E$, and a constant 15 mA/m current tailward of $120 R_E$ [Slavin et al., 1985]. Thus, at large distances the observed lobe field values are between the small T89 values and the simulation results.

The $B_Z$ profiles for pure dipole field, for the T89 ($Kp = 2$) model, and for both simulations shown in Figure 1c are presented in Figure 1d. In the T89 model the strong currents lead to very small $B_Z$ along the tail axis at and tailward of $15 R_E$. In the simulation for northward IMF the current sheet is relatively thin, and the weak near-Earth currents lead to small $B_Z$ around $20 R_E$. In a limited section close to midnight, a neutral line remains stationary inside $30 R_E$. In the simulation with the variable, more realistic, northward IMF, the current sheet is much thicker and $B_Z$ is relatively large (almost 10 nT) throughout the mid-tail and distant tail.

## Substorm development

During the substorm growth phase the lobe field increases and the equatorial field strength decreases, the changes being strongest near the midnight sector of the near-Earth tail [e.g., Baker and Pulkkinen, 1991]. Figure 2a shows an empirically derived model for the cross-tail current enhancement during the substorm growth phase ($AE_{MAX} \simeq 500$ nT; Event 1 in [Pulkkinen et al., 1992]). The model was based on temporally-evolving modifications implemented within the T89 ($Kp = 2$) model. The substorm-associated parameters were evaluated by fitting multiple spacecraft observations of the near-tail magnetic field during the growth phase. Note the strong enhancement of the currents in the near-Earth region in addition to slight enhancement throughout the tail from the beginning of the growth phase ($t = 0$) to substorm onset 70 min later.

Figure 2b shows the integrated current during several time steps of the substorm evolution in the MHD simulation by Raeder [1994]. The three solid curves show the evolution from the quiet time configuration to the

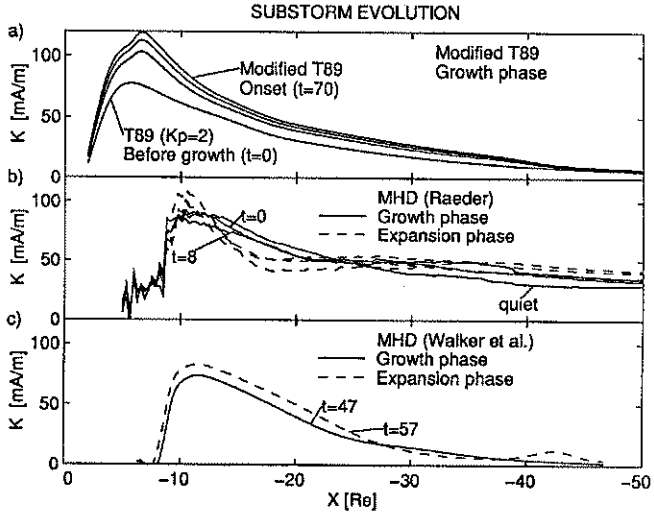


**Figure 2** a) Integrated currents at $Y = 0$ during the substorm growth phase from the empirical model by Pulkkinen et al. [1992], b) from the MHD simulation by Raeder [1994], and c) from the MHD simulation by Walker et al. [1993].

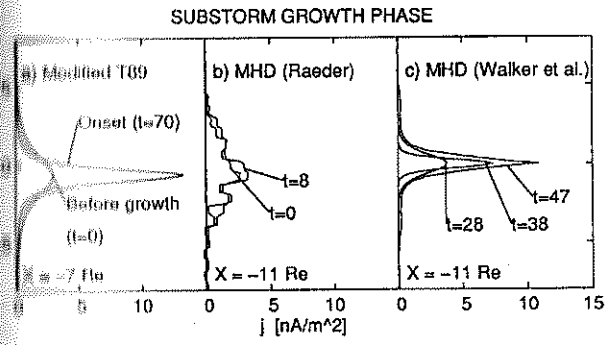


Figure 3 Current density as a function of distance from the current sheet center (a) from the empirical model by Pulkkinen et al. [1992], (b) from the MHD simulation by Raeder [1994], and c) from the MHD simulation by Walker et al. [1993].

substorm onset ($t = 8$ min). In the simulations, the substorm growth phase ($t = 0$) is defined to begin when the IMF turns southward, and the onset is taken to be the time when fast reconnection begins in the near-Earth tail. The dashed lines show the currents during the expansion phase (at 18, 26, and 35 min). Note that here the current enhancement during the growth phase is much smaller and takes place mainly outside $25R_E$. The stretching signatures near geostationary orbit suggested both by observations [e.g., Baker and McPherron, 1990] and by empirical modeling [e.g., Pulkkinen et al., 1992] are not present in this simulation. Figure 2c shows the current distribution at the end of the growth phase ($t = 47$ min) and during the expansion phase ($t = 57$ min) from a simulation by Walker et al. [1993] ($B_y = -5$ nT, $V_X = 300$ km/s, $n = 5\text{cm}^{-3}$, $T = 3 \cdot 10^5$ K). In this simulation the increase of the tail current during the growth phase was larger than in the Raeder [1994] simulation (not shown), and the growth phase lasted much longer.

Extreme thinning of the near-tail current sheet during the growth phase has been observed [e.g., Baker and McPherron, 1990] and was also suggested by the empirical model [Pulkkinen et al., 1992]. Figure 3a shows the current density profiles at the location of the peak current intensity for the empirical model in Figure 2a. Note how the peak intensity increases strongly as the current sheet thins during the growth phase. Even stronger thinning has been found in the empirical modeling in connection with substorms during stronger activity [Pulkkinen et al., 1992].

In the Raeder [1994] simulation the current sheet is relatively thick, and consequently the current density is not very high (Figure 3b). During the growth phase the peak intensity slightly increases, but there is little variation in the current sheet thickness. The largest changes in the current sheet structure are associated with the plasmoid during the expansion phase. The Walker et al. [1993] simulation (Figures 2c and 3c) shows a much stronger current maximum increase at the end of the growth phase ($t = 47$ min). Due to problems with the data tapes, the earlier time steps could not be recovered. From the available maximum current density values and the plasma pressure values the approximate current sheet thicknesses could be estimated. The earlier time steps (28 and 38 min) shown are plotted by using model current sheet profiles ($j_0/cosh^2(Z/D)$) using the known maximum current densities ($j_0$) and the estimated current sheet thicknesses ($D$).

The dashed curves in Figures 2b and 2c show the integrated current during the expansion phase in the MHD simulations. The current intensity in the near-Earth tail increases rather than decreases after the onset of reconnection. Furthermore, there is little time variation during the expansion phase. Similarly, the current density (not shown) at the tail center is also at a maximum throughout the expansion phase. The lack of current disruption may be caused by the large size of the ionosphere ($\sim 3.5R_E$) in the simulations. This could lead to unrealistically large plasma pressure and increase of the local current density near the Earth. Or, the current intensity may stay at a high level due to continuous driving by the southward IMF [Ogino et al., 1994]. Obviously, further work is required to resolve this issue.

## Summary and Discussion

We have compared global MHD simulation runs by Walker et al. [1993], Raeder et al. [1994] and Raeder, [1994] and empirical magnetic field models [Tsyganenko, 1989]. We have also utilized variants of the empirical models for the substorm growth phase [Pulkkinen et al., 1992]. The following summarizes our main results:

1) The radial current profiles produced by the empirical models and MHD simulations reveal considerable differences. Whereas the empirical models successfully describe the inner tail strong currents, the MHD models give a more accurate representation in the mid-tail.

2) The MHD models do not include the effects of the near-Earth ring current. The inner edge of the cross-tail current in the MHD models is at $\sim 8R_E$, and the observed relatively strong currents inside that distance present in the T89 models are entirely absent in the MHD solutions.

3) During the substorm growth phase (southward IMF) the empirical models predict strong enhancement of the near-tail currents. The MHD simulations also show a slight increase in the current, but the enhancement takes place further out. Furthermore, comparison of the two MHD simulations shows that the duration of the growth phase is strongly dependent on the initial conditions in the tail [Walker et al., 1993].

4) During the expansion phase the onset of reconnection and the formation of a plasmoid does not lead to the disruption of the cross-tail currents in the MHD models. Both the current density and the total current strength continue to increase during the expansion phase.

At present the regions of best validity of the MHD simulations and empirical models are complementary: The empirical models are best in the inner tail, where the density of data points used to create the models is largest. On the other hand, the MHD models are most

reliable outside the region where the large field gradients require very small grid size. Therefore, further intercomparison of the current distributions can lead to improvements in both types of models. Whereas the MHD models can serve as an "additional data base" to the empirical models, the empirical models can be used as initial conditions in the MHD simulations. Although the details of the discrepancies may be attributed to different initial conditions in the simulation runs or details of the simulation codes, the main features pointed out in this paper are characteristic of a number of empirical models and simulations, most likely caused by differences in the modeling approaches.

Using empirical and global MHD models concurrently to model the substorm cycle promises to give important clues on how the different processes in the magnetotail interact and lead to the observed features. Because the instability development is critically dependent on the field and current values along the tail axis, finding the correct representation for the tail field during the late growth phase is of key importance. For example, formation of the current maximum outside the near-tail region characterized by strong field gradients in the $X$-direction and relatively large $B_Z$ values may cause changes in timing and nature of the instability development. Thus, the MHD models need to be improved to include the physical processes that cause the extreme stretching of the near-tail flux tubes during the growth phase, otherwise it will be difficult to model the current sheet instability and substorm energy release.

The Tsyganenko models are established by averaging data collected under much varying solar wind conditions, which may cast doubt that the final configuration does not represent a true instantaneous magnetospheric configuration or a true MHD equilibrium state. However, Hesse and Birn [1993] have shown that the quiet Tsyganenko tail magnetic field is very close to a self-consistent equilibrium state arrived at in their MHD tail simulations. Moreover, the empirical modeling by Pulkkinen et al. [1992] represents quite consistently the observations from several spacecraft in the near-Earth tail, and the highly stretched configuration prior to substorm onset can also be represented by an MHD equilibrium state [Hesse et al., 1994]. The fidelity of these modeling fits for specific events suggests that the essential self-consistent pressure equilibrium has been captured in the empirical model efforts.

At the present stage it is important to determine to which degree the simulation schemes can be improved to include the observed features, and what is the significance of the non-MHD processes to the global dynamical evolution of the magnetosphere.

**Acknowledgments.** This work was initiated while TP was visiting UCLA under the auspices of NASA Goddard Space Flight Center. The hospitality of UCLA is gratefully acknowledged. The work at UCLA has been supported by the Solar Terrestrial Physics program under NASA grant NAG-5 1100. We thank T. Ogino for the Walker et al. simulations and J. Berchem for fruitful discussions.

## References

Baker, D. N. and R. L. McPherron, Extreme energetic particle decreases near geostationary orbit: A manifestation of current diversion within the inner plasma sheet, *J. Geophys. Res., 95*, 6591, 1990.

Baker, D. N., and T. I. Pulkkinen, The Earthward edge of the plasma sheet in magnetospheric substorms, in J. R. Kan, T. A. Potemra, S. Kokubun, and T. Iijima (eds): *Magnetospheric substorms*, Geophysical Monograph 64, 147, AGU, Washington D.C., 1991.

Hesse, M. and J. Birn, Three-dimensional magnetotail equilibria by numerical relaxation techniques. *J. Geophys. Res., 98*, 3973, 1993.

Hesse, M., J.Birn, D. N. Baker, and T. I. Pulkkinen, MHD simulations of substorm dynamics including an inner magnetotail, *Proceedings of the 2nd International Conference on Substorms*, Fairbanks, Alaska, in press, 1994.

Ogino, T., R. J. Walker, and M. Ashour-Abdalla, A global magnetohydrodynamic simulation of steady magnetospheric convection, *Proceedings of the 2nd International Conference on Substorms*, Fairbanks, Alaska, in press, 1995.

Pulkkinen, T. I., D. N. Baker, R. J. Pellinen, J. Büchner, H. E. J. Koskinen, R. E. Lopez, R. L. Dyson, and L. A. Frank, Particle scattering and current sheet stability in the geomagnetic tail during the substorm growth phase. *J. Geophys. Res., 97*, 19283, 1992.

Raeder, J., R. J. Walker, and M. Ashour-Abdalla, The structure of the distant geomagnetic tail during long periods of northward IMF. *Geophys. Res. Lett., in press*, 1995.

Raeder, J., Global MHD simulations of the dynamics of the magnetosphere: Weak and strong solar wind forcing. *Proceedings of the 2nd International Conference on Substorms*, Fairbanks, Alaska, in press, 1995.

Slavin, J. A., E. J. Smith, D. G. Sibeck, D. N. Baker, R. D. Zwickl, and S.-I. Akasofu, An ISEE-3 study of average and substorm conditions in the distant magnetotail, *J. Geophys. Res., 90*, 10,875, 1985.

Tsyganenko, N. A., Magnetospheric magnetic field model with a warped tail current sheet. *Planet. Space Sci., 37*, 5, 1989.

Walker, R. J., T. Ogino, J. Raeder, and M. Ashour-Abdalla, A global magnetohydrodynamic simulation of the magnetosphere when the interplanetary magnetic field is southward: The onset of magnetotail reconnection. *J. Geophys. Res., 98*, 17235, 1993.

T. I. Pulkkinen, Finnish Meteorological Institute, P.O.Box 503, FIN-00101 Helsinki, Finland, Internet: tuija.pulkkinen@fmi.fi

D. N. Baker, NASA Goddard Space Flight Center, Greenbelt, MD 20771.

R. J. Walker, J. Raeder, and M. Ashour-Abdalla, Institute of Geophysics and Planetary Physics, University of California, Los Angeles, CA 90024.

(received 10 August 1994; revised 3 January 1995; accepted 31 January 1995.)